

A constitutively open potassium channel formed by KCNQ1 and KCNE3

Björn C. Schroeder^{*†}, Siegfried Waldegger^{*†}, Susanne Fehr^{*},
Markus Bleich[‡], Richard Warth[‡], Rainer Greger[‡] & Thomas J. Jentsch^{*}

^{*} Zentrum für Molekulare Neurobiologie Hamburg (ZMNH),
Hamburg University, Martinistrasse 85, D-20246 Hamburg, Germany

[‡] Physiologisches Institut der Albert-Ludwigs-Universität Freiburg,
Hermann-Herder-Strasse 7, D-79104 Freiburg, Germany

[†] These authors contributed equally to this work

Mutations in all four known KCNQ potassium channel α -subunit genes lead to human diseases^{1–6}. KCNQ1 (KvLQT1)¹ interacts with the β -subunit KCNE1 (IsK, minK)⁷ to form the slow, depolarization-activated potassium current I_{Ks} ^{8,9} that is affected in some forms of cardiac arrhythmia. Here we show that the novel β -subunit KCNE3 markedly changes KCNQ1 properties to yield currents that are nearly instantaneous and depend linearly on voltage. It also suppresses the currents of KCNQ4 and HERG potassium channels. In the intestine, KCNQ1 and KCNE3 messenger RNAs colocalized in crypt cells. This localization and the pharmacology, voltage-dependence and stimulation by cyclic AMP of KCNQ1/KCNE3 currents indicate that these proteins may assemble to form the potassium channel that is important for cyclic AMP-stimulated intestinal chloride secretion and that is involved in secretory diarrhoea and cystic fibrosis.

KCNQ proteins have six transmembrane domains and probably function as tetramers. In the heart and in the cochlea, KCNQ1 associates with KCNE1, a small protein which spans the membrane only once⁷. Dominant mutations in either KCNQ1 (refs 10, 11) or KCNE1 (ref. 12) prolong cardiac action potentials in long-QT syndrome. A total loss of function additionally causes deafness² by impairing potassium secretion across the stria vascularis of the cochlea. The positive apical membrane potential of these cells¹³ allows KCNQ1/KCNE1 channels to be open. KCNQ1 is also expressed in several other tissues¹⁰, but its role in these organs is unclear. Pharmacological data have indicated that KCNQ1 may be important for chloride secretion in the colon¹⁴. However, the negative membrane voltage of intestinal epithelial cells would prevent KCNQ1 or KCNQ1/KCNE1 from being open. This suggests that there may be another subunit.

We cloned the β -subunit KCNE3 (ref. 15) by homology to KCNE1. It is a 103-amino-acid protein with a relative molecular mass of ~12,000 ($M_r \approx 12K$) that displays roughly 35% identity to other KCNE proteins within the single transmembrane domain and a following short stretch (Fig. 1). Northern analysis revealed a prominent band in the kidney, moderate expression in the small intestine and weaker bands in most other tissues including colon and heart (see Supplementary Information).

We co-expressed KCNE3 with KCNQ1 through KCNQ4. KCNQ1

gave potassium currents that slowly activated at potentials more positive than -40 mV (Fig. 2a). Co-expression with KCNE1 enhanced the current amplitudes, slowed channel activation and shifted the voltage dependence to more positive potentials^{8,9} (Fig. 2b). Co-expression with KCNE3 caused a marked change in the channel properties (Fig. 2c, d). Currents now had a linear I/V relationship, were also present at negative voltages and were nearly instantaneous. There was some time-dependent gating at positive voltages. Ion substitution experiments showed that the KCNQ1/KCNE3 channel is highly selective for potassium (Fig. 2e). Co-expression of KCNQ1 with KCNE1 and KCNE3 gave currents that could not be distinguished from a linear superposition of KCNQ1/KCNE1 and KCNQ1/KCNE3 channels (data not shown). KCNQ1 currents are specifically inhibited by chromanol 293B, and the sensitivity of KCNQ1/KCNE1 heteromers is increased¹⁶ by a factor of ~10. Chromanol 293B at $10 \mu M$ inhibited KCNQ1 channels by ~20%, and this inhibition was increased to ~85% when KCNE3 was co-expressed (Fig. 2f). KCNQ1/KCNE3 channels were inhibited by chromanol 293B with an inhibitory constant $K_i \approx 3 \mu M$ (Fig. 2g). KCNE3 also increased the sensitivity to clotrimazole, an inhibitor of distinct calcium- and cAMP-activated potassium channels^{17,18} (Fig. 2f). Barium (5 mM) inhibited KCNQ1/KCNE3 currents by ~70% (data not shown). Like KCNQ1 (ref. 19) and KCNQ2/KCNQ3 heteromers²⁰, KCNQ1/KCNE3 currents were enhanced by increasing intracellular cAMP (Fig. 2h). To confirm that KCNQ1 and KCNE3 interact physically, we transfected epitope-tagged versions of both subunits into mammalian cells. Immunofluorescence showed that KCNQ1 resided in the plasma membrane irrespective of whether it was co-expressed with KCNE3. However, KCNE3 was distributed in small vesicles in the cytoplasm when expressed alone (Fig. 3a), but was transported to the plasma membrane where it colocalized with KCNQ1 when they were expressed together (Fig. 3b, c). Also, in *Xenopus* oocytes, co-injection with KCNQ1 greatly increased surface expression²¹ of KCNE3 (Fig. 3d).

In contrast, currents from KCNQ2/KCNQ3 channels (which are mutated in neonatal epilepsy²⁰) were not significantly affected by the same level of KCNE3 expression (Fig. 4a, b). Currents from KCNQ4, a channel that is mutated in dominant deafness⁶, were largely suppressed by KCNE3 (Fig. 4c, d). Currents of the HERG potassium channel are also modulated by KCNE1 (ref. 22) and KCNE2 (ref. 15). Co-expression of KCNE3 strongly inhibited HERG currents (Fig. 4e, f).

As KCNE3 expression in heart is weak compared with those of HERG²³ and KCNE1 (ref. 10), it is unclear whether the effect on HERG is physiologically important. *In situ* hybridization of cochlear sections with a KCNE3 probe revealed no specific signal (J. P. Hardelin and C. Petit, personal communication), indicating that it may not suppress KCNQ4 currents in sensory outer hair cells⁶.

The interaction with KCNQ1, however, is highly significant. KCNE3 and KCNQ1 are expressed together in various tissues, including the small intestine, colon and kidney^{10,19}. The KCNQ1/KCNE3 channel

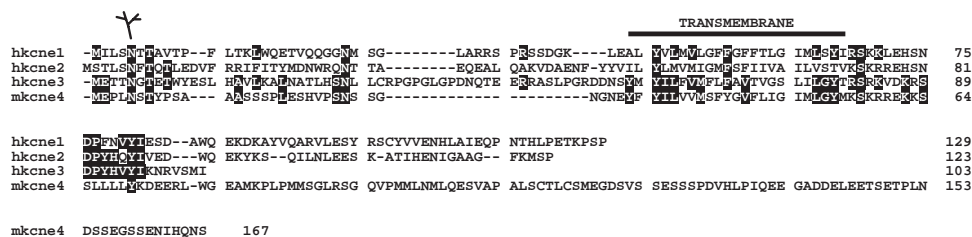


Figure 1 Primary structure of KCNE3. Amino-acid sequence comparison of human KCNE3 (third line) with other KCNE proteins. Black background indicates residues that are identical in KCNE3 and at least one other KCNE protein. The bar indicates the predicted transmembrane domain. There is a conserved consensus site for *N*-glycosylation near the

amino terminus, as indicated by the branched symbol. It is likely that all these proteins have an extracellular N terminus, as also supported by the experiment shown in Fig. 3d. Accession numbers are M26685, KCNE1; AF071002, KCNE2; AF076531, KCNE3; AF076533, KCNE4 (ref. 17).

is open at resting potentials and is therefore suitable for mediating transepithelial transport. Several reports stress the importance of a basolateral potassium conductance in cAMP-stimulated secretion of chloride by colonic crypt cells^{17,18,24–28}. This channel is thought to recycle potassium that is transported into the cell by the basolateral NaK2Cl cotransporter. It thereby stimulates basolateral uptake of chloride and hyperpolarizes the cell. Both effects increase the driving force for the apical exit of chloride ions through the CFTR chloride channel. The basolateral cAMP-dependent potassium conductance was sensitive^{14,27,28} to chromanol 293B, a specific inhibitor of KCNQ1/KCNE1 (ref. 16). However, the voltage dependence of KCNQ1 (and KCNQ1/KCNE1) channels predicts that they would be closed at resting voltages. It also differs from the voltage dependence of chromanol-sensitive potassium currents in native intestinal crypt cells²⁹. The chromanol-sensitive component of potassium currents is instantaneous, has a linear *I/V* relationship and is enhanced by intracellular cAMP (Fig. 5). It is also inhibited by clotrimazole (data not shown). A similar linear *I/V* relationship was

observed for a cAMP-activated, clotrimazole-sensitive, basolateral potassium conductance in apically permeabilized T84 colon carcinoma cell monolayers¹⁸.

Our work indicates that KCNQ1/KCNE3 may be the molecular basis of this colonic channel. KCNE3 renders KCNQ1 a constitutively open channel with a linear *I/V* relationship. KCNQ1/KCNE3 channels share many other features with the native current of colonic crypt cells: both are stimulated by cAMP^{17,18,25–28} and are sensitive to micromolar amounts of chromanol 293B^{24–28}. In the human colon, chromanol 293B inhibited cAMP-stimulated secretion of chloride with a similar inhibitory constant ($K_i \approx 5 \mu\text{M}$)²⁶ as that with which it inhibited human KCNQ1/KCNE3 in *Xenopus* oocytes ($\sim 3 \mu\text{M}$; Fig. 2g). Both currents are also inhibited by clotrimazole, which blocks both cAMP- and calcium-stimulated

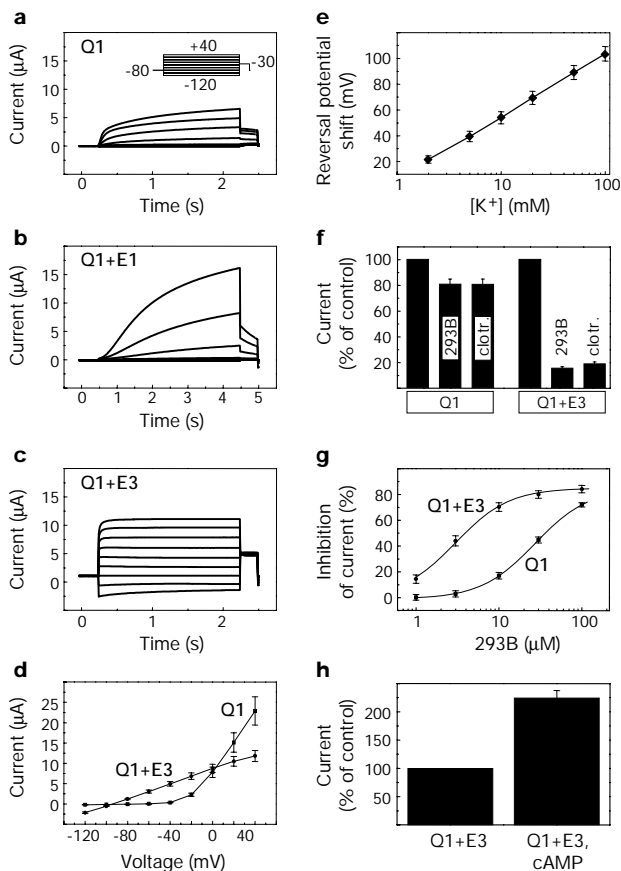


Figure 2 Modification of KCNQ1 currents by KCNE1 and KCNE3. Two-electrode voltage clamp traces of *Xenopus* oocytes injected with cRNA encoding KCNQ1 (a), KCNQ1 and KCNE1 (b) and KCNQ1 and KCNE3 (c). Voltage was clamped between -120 and $+40$ mV (a, inset). Longer pulses were used in b, d. Averaged current/voltage relationships for KCNQ1 (squares) and KCNQ1/KCNE3 (circles). Currents obtained after 2 s at the respective voltages were averaged from 13 oocytes. e–h, Characterization of KCNQ1/KCNE3 currents. e, Shift of reversal potential as a function of extracellular K^+ concentration (53 mV per decade). Results are from 15 oocytes from two different batches. f, Effect of chromanol 293B ($10 \mu\text{M}$) and clotrimazole (clotr.; $20 \mu\text{M}$) on KCNQ1/KCNE3 and KCNQ1 (averaged from ≥ 5 oocytes). g, Dose–response curve for chromanol 293B of KCNQ1 (squares) and KCNQ1/KCNE3 (circles) channels. Currents were measured after 2 s at clamping to $+40$ mV and averaged from six oocytes. This yields $K_i \approx 27 \mu\text{M}$ for KCNQ1 and $K_i \approx 3 \mu\text{M}$ for KCNQ1/KCNE3. h, Effect of raising intracellular cAMP on KCNQ1/KCNE3 currents. Results are from 10 oocytes from two different batches. Error bars indicate s.e.m. throughout.

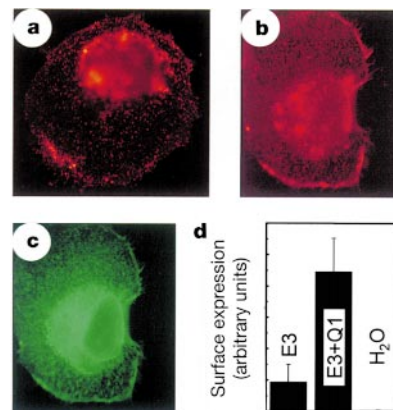


Figure 3 Stimulation of KCNE3 surface expression by KCNQ1. a, KCNE3 is localized in numerous intracellular vesicles in a CHO cell transfected with epitope-tagged KCNE3. b, Surface staining for KCNE3 in a CHO cell cotransfected with KCNQ1. c, The same cell stained for KCNQ1. As is common with overexpression of membrane proteins, there is also labelling of intracellular structures which may correspond to the endoplasmic reticulum and Golgi. d, Surface expression of epitope-tagged KCNE3 in *Xenopus* oocytes using a luminescence detection method²¹. The surface expression of KCNE3 in the absence of exogenous KCNQ1 may be due to κKCNQ1 endogenous to *Xenopus* oocytes⁹. Mean values from 15 oocytes are shown, with error bars indicating s.e.m.

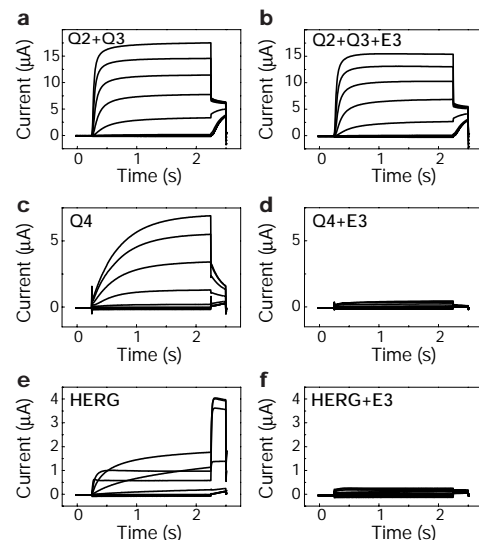


Figure 4 Effect of KCNE3 on other channels. a, b, Effects on KCNQ2/KCNQ3 heteromers; c, d, effects on KCNQ4; e, f, effects on HERG. Two-electrode voltage clamp measurements of *Xenopus* oocytes, using the clamp protocol of inset in Fig. 2a. Currents were averaged from more than seven oocytes. KCNE3 was co-injected in b, d, f, but was lacking in a, c, e.

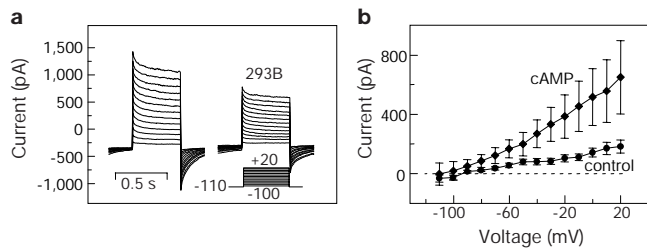


Figure 5 Chromanol 293B-sensitive currents in rat colonic crypt cells. **a**, Whole-cell voltage-clamp traces before and after addition of 10 μ M chromanol 293B. From a holding potential of -110 mV, the voltage was clamped for 500 ms to values between -100 and $+20$ mV. The channels were activated by raising intracellular cAMP using 10 μ M forskolin and 100 μ M 8-CPT-cAMP, and were measured in the absence of Cl^- and the presence of 10 nM charybdotoxin to inhibit Cl^- channels and Ca^{2+} -activated K^+ channels, respectively. Chromanol-sensitive currents showed no time-dependent relaxations even with pulses of 2 s (not shown). **b**, Current/voltage relationship of chromanol-sensitive current before and after adding forskolin/cAMP.

intestinal chloride secretion^{17,18} and which can block cholera-toxin-induced diarrhoea in animals¹⁸.

In situ hybridization revealed both KCNQ1 and KCNE3 in crypt cells of the small intestine and the colon (Fig. 6a–f). Consistent with the finding that crypts are the predominant site of cAMP-stimulated chloride and fluid secretion, expression of both KCNQ1 and KCNE3 decreased along the crypt–villus axis and paralleled that of the CFTR chloride channel³⁰. Importantly, cAMP-activated secretion of chloride ions in the jejunum is also inhibited by chromanol 293B (data not shown). Northern analysis revealed that both KCNQ1 and KCNE3, but not KCNE1, are expressed in T84 colonic epithelial cells (Fig. 6g). These cells are a useful model system to study the importance of basolateral potassium channels in chloride secretion^{17,18,25} and express the cAMP-activated channel that is sensitive to chromanol and clotrimazole. By contrast, HEK293 kidney cells do not express these proteins.

Our work shows an unexpected effect on the gating of KCNQ1 of

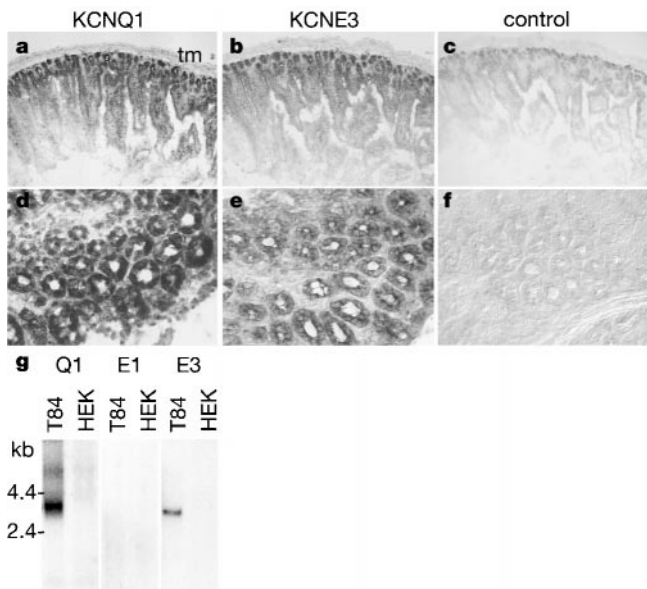


Figure 6 Localization of KCNQ1 and KCNE3 in the mouse small intestine and colon by *in situ* hybridization. **a–c**, Small intestine sections hybridized with a KCNQ1 antisense probe (**a**), a KCNE3 antisense probe (**b**) and a KCNQ1 sense probe as a control (**c**). tm, tunica muscularis. **d–f**, Colon crypts hybridized to KCNQ1 (**d**) and KCNE3 (**e**) antisense probes, and a KCNE3 sense probe (**f**) as negative control. **g**, Northern analysis of T84 human colon epithelial cells and HEK293 human embryonic kidney cells for expression of KCNQ1, KCNE1 and KCNE3. 25 μ g total RNA was loaded per lane.

a protein with a single transmembrane domain. It differs fundamentally from the effect of the structurally related KCNE1 subunit, promising interesting insight into mechanism of channel gating. Furthermore, our results indicate that KCNQ1 and KCNE3 may form the cAMP-activated potassium channel that participates in cAMP-stimulated intestinal secretion of chloride ions, which is reduced in cystic fibrosis and pathologically stimulated in cholera and other forms of secretory diarrhoea. The rather broad and partially overlapping tissue distributions of KCNQ1 and KCNE3 indicate that KCNQ1/KCNE3 channels may exert similar functions in other tissues as well. □

Methods

Cloning and functional expression of KCNE3

KCNE3 was cloned by PCR on a clone from human colon complementary DNA (accession no. AA133012) which we identified by a BLAST search of the dBEST database using the KCNE2 sequence that we had identified by homology to KCNE1. The KCNE3 sequence has been deposited into the database¹⁵, but no effects on KCNQ and HERG channels had been detected. The KCNE3 cDNA was inserted into vector pTLN⁶. From this clone (1 ng per oocyte) and from KCNQ and HERG clones (10 ng per oocyte, respectively) was synthesized and expressed and measured in *Xenopus* oocytes as described⁶. In most cases, KCNE3 injection by itself gave no currents. Sometimes there were small currents that may have been due to an interaction with the xKvLQT1 protein that is endogenous to *Xenopus* oocytes⁹.

Measurements were performed in ND96 (96 mM NaCl, 2 mM KCl, 1.8 mM CaCl_2 , 1 mM MgCl_2 , 5 mM HEPES pH 7.4). In Fig. 2d, KCl was exchanged for equivalent amounts of NaCl. Chromanol 293B²⁴ was added from a 10 mM stock, and clotrimazole from a 100 mM stock (both in DMSO). Intracellular cAMP was raised in *Xenopus* oocytes by applying 1 mM IBMX and 10 μ M forskolin ≥ 10 min.

Localization of KCNE3 and KCNQ1

In situ hybridization was performed on cryosections of mouse small intestine and colon using mouse KCNQ1 and KCNE3 antisense and sense cRNAs in the DIG labelling system (Roche). For immunodetection, KCNQ1 and KCNE3 were tagged at the amino terminus with the FLAG- and HA-epitope, respectively, subcloned into pCDNA3, and transfected into CHO cells. After two days, cells were studied by immunofluorescence using monoclonal antibodies against these epitopes and secondary antibodies labelled with Cy2 and Cy3. To determine surface expression of KCNE3 in oocytes, we used HA-tagged KCNE3 and untagged KCNQ1 and the enzymatic detection system as described²¹.

Patch-clamp analysis of colonic crypt cells

We prepared colonic crypts as described²⁸ and performed whole-cell patch clamp measurements. Cells were held at their membrane voltage and a clamp protocol was applied every 15 s as indicated in Fig. 5. Patch pipettes were filled with 95 mM K-gluconate, 30 mM KCl, 1.2 mM $\text{Na}_2\text{H}_2\text{PO}_4$, 4.8 mM Na_2HPO_4 , 0.73 mM Ca-gluconate, 1 mM MgCl_2 , 1 mM EGTA, 5 mM D-glucose and 3 mM ATP. The bath solution contained 145 mM Na-gluconate, 1.6 mM K_2HPO_4 , 0.4 mM KH_2PO_4 , 8 mM Ca-gluconate, 1 mM MgSO_4 and 5 mM D-glucose. cAMP was raised by applying 5 μ M forskolin and 100 μ M 8-CPT cAMP to the bath. In some experiments the Ca^{++} -activated K^+ -channel was additionally inhibited by 5 nM charybdotoxin.

Received 19 October; accepted 24 November 1999.

- Wang, Q. *et al.* Positional cloning of a novel potassium channel gene: KVLQT1 mutations cause cardiac arrhythmias. *Nature Genet.* **12**, 17–23 (1996).
- Neyroud, N. *et al.* A novel mutation in the potassium channel gene KVLQT1 causes the Jervell and Lange-Nielsen cardioauditory syndrome. *Nature Genet.* **15**, 186–189 (1997).
- Bievart, C. *et al.* A potassium channel mutation in neonatal human epilepsy. *Science* **279**, 403–406 (1998).
- Singh, N. A. *et al.* A novel potassium channel gene, KCNQ2, is mutated in an inherited epilepsy of newborns. *Nature Genet.* **18**, 25–29 (1998).
- Charlier, C. *et al.* A pore mutation in a novel KQT-like potassium channel gene in an idiopathic epilepsy family. *Nature Genet.* **18**, 53–55 (1998).
- Kubisch, C. *et al.* KCNQ4, a novel potassium channel expressed in sensory outer hair cells, is mutated in dominant deafness. *Cell* **96**, 437–446 (1999).
- Takumi, T., Ohkubo, H. & Nakanishi, S. Cloning of a membrane protein that induces a slow voltage-gated potassium current. *Science* **242**, 1042–1045 (1988).
- Barhanin, J. *et al.* KvLQT1 and IsK (minK) proteins associate to form the I_{Ks} cardiac potassium current. *Nature* **384**, 78–80 (1996).
- Sanguinetti, M. C. *et al.* Coassembly of KvLQT1 and minK (IsK) proteins to form cardiac I_{Ks} potassium channel. *Nature* **384**, 80–83 (1996).
- Chouabe, C. *et al.* Properties of KvLQT1 K^+ channel mutations in Romano-Ward and Jervell and Lange-Nielsen inherited cardiac arrhythmias. *EMBO J.* **16**, 5472–5479 (1997).
- Wollnik, B. *et al.* Pathophysiological mechanisms of dominant and recessive KvLQT1 K^+ channel mutations found in inherited cardiac arrhythmias. *Hum. Mol. Genet.* **6**, 1943–1949 (1997).
- Splawski, I., Tristani-Firouzi, M., Lehmann, M. H., Sanguinetti, M. C. & Keating, M. T. Mutations in the hminK gene cause long QT syndrome and suppress I_{Ks} function. *Nature Genet.* **17**, 338–340 (1997).
- Offner, F. F., Dallos, P. & Cheatham, M. A. Positive endocochlear potential: mechanism of production by marginal cells of stria vascularis. *Hear. Res.* **29**, 117–124 (1987).

14. Suessbrich, H. Specific blockade of slowly activating I_{Ks} channels by chromanol—impact on the role of I_{Ks} channels in epithelia. *FEBS Lett.* **396**, 271–275 (1996).
15. Abbott, G. W. *et al.* MiRP1 forms I_{Ks} potassium channels with HERG and is associated with cardiac arrhythmia. *Cell* **97**, 175–187 (1999).
16. Busch, A. E. *et al.* The role of the I_{Ks} protein in the specific pharmacological properties of the I_{Ks} channel complex. *Br. J. Pharmacol.* **122**, 187–189 (1997).
17. Devor, D. C., Singh, A. K., Gerlach, A. C., Frizzell, R. A. & Bridges, R. J. Inhibition of intestinal Cl^- secretion by clotrimazole: direct effect on basolateral membrane K^+ channels. *Am. J. Physiol.* **273**, C531–C540 (1997).
18. Rufo, P. A. *et al.* The antifungal antibiotic, clotrimazole, inhibits chloride secretion by human intestinal T84 cells via blockade of distinct basolateral K^+ conductances. Demonstration of efficacy in intact rabbit colon and in an *in vivo* mouse model of cholera. *J. Clin. Invest.* **100**, 3111–3120 (1997).
19. Yang, W. P. *et al.* KvLT1, a voltage-gated potassium channel responsible for human cardiac arrhythmias. *Proc. Natl Acad. Sci. USA* **94**, 4017–4021 (1997).
20. Schroeder, B. C., Kubisch, C., Stein, V. & Jentsch, T. J. Moderate loss of function of cyclic-AMP-modulated $KCNQ2/KCNQ3$ K^+ channels causes epilepsy. *Nature* **396**, 687–690 (1998).
21. Zerangue, N., Schwappach, B., Jan, Y. N. & Jan, L. Y. A new ER trafficking signal regulates the subunit stoichiometry of plasma membrane K_{ATP} channels. *Neuron* **22**, 537–548 (1999).
22. McDonald, T. V. *et al.* A minK-HERG complex regulates the cardiac potassium current I_{Kr} . *Nature* **388**, 289–292 (1997).
23. Curran, M. E. *et al.* A molecular basis for cardiac arrhythmia: HERG mutations cause long QT syndrome. *Cell* **80**, 795–803 (1995).
24. Lohrmann, E. *et al.* A new class of inhibitors of cAMP-mediated Cl^- secretion in rabbit colon, acting by the reduction of cAMP-activated K^+ conductance. *Pflügers Arch.* **429**, 517–530 (1995).
25. Devor, D. C., Singh, A. K., Frizzell, R. A. & Bridges, R. J. Modulation of Cl^- secretion by benzimidazolones. I. Direct activation of a Ca^{2+} -dependent K^+ channel. *Am. J. Physiol.* **271**, L775–L784 (1996).
26. Mall, M. *et al.* Cholinergic ion secretion in human colon requires coactivation by cAMP. *Am. J. Physiol.* **275**, G1274–G1281 (1998).
27. MacVinish, L. J., Hickman, M. E., Mufti, D. A., Durrington, H. J. & Cuthbert, A. W. Importance of basolateral K^+ conductance in maintaining Cl^- secretion in murine nasal and colonic epithelia. *J. Physiol. (Lond.)* **510**, 237–247 (1998).
28. Warth, R. *et al.* The cAMP-regulated and 293B-inhibited K^+ conductance of rat colonic crypt base cells. *Pflügers Arch.* **432**, 81–88 (1996).
29. Diener, M., Hug, F., Strabel, D. & Scharrer, E. Cyclic AMP-dependent regulation of K^+ transport in the rat distal colon. *Br. J. Pharmacol.* **118**, 1477–1487 (1996).
30. Trezise, A. E. & Buchwald, M. *In vivo* cell-specific expression of the cystic fibrosis transmembrane conductance regulator. *Nature* **353**, 434–437 (1991).

Supplementary information is available on Nature's World-Wide Web site (<http://www.nature.com>) or as paper copy from the London editorial office of Nature.

Acknowledgements

We thank J. P. Hardelin and C. Petit for performing KCNE3 *in situ* hybridization of cochlear sections. This work was supported by grants from the Deutsche Forschungsgemeinschaft and the Fonds der Chemischen Industrie to R.G. and T.J.J.

Correspondence and requests for materials should be addressed to T.J.J. (e-mail: jentsch@plexus.uke.uni-hamburg.de).

Uptake of apoptotic cells drives the growth of a pathogenic trypanosome in macrophages

Célio G. Freire-de-Lima*, Danielle O. Nascimento*, Milena B. P. Soares†, Patricia T. Bozza‡, Hugo C. Castro-Faria-Neto‡, Fernando G. de Mello*, George A. DosReis* & Marcela F. Lopes*

* Instituto de Biofísica Carlos Chagas Filho, Universidade Federal do Rio de Janeiro, 21944-970, Rio de Janeiro, RJ, Brazil

† Centro de Pesquisas Gonçalo Moniz, FIOCRUZ, 40295-001, Salvador, BA, Brazil

‡ Instituto Oswaldo Cruz, FIOCRUZ, 21045-900, Rio de Janeiro, RJ, Brazil

After apoptosis, phagocytes prevent inflammation and tissue damage by the uptake and removal of dead cells¹. In addition, apoptotic cells evoke an anti-inflammatory response through macrophages^{2,3}. We have previously shown that there is intense lymphocyte apoptosis in an experimental model of Chagas' disease⁴, a debilitating cardiac illness caused by the protozoan *Trypanosoma cruzi*. Here we show that the interaction of apoptotic,

but not necrotic T lymphocytes with macrophages infected with *T. cruzi* fuels parasite growth in a manner dependent on prostaglandins, transforming growth factor- β (TGF- β) and polyamine biosynthesis. We show that the vitronectin receptor is critical, in both apoptotic-cell cytoadherence and the induction of prostaglandin E_2 /TGF- β release and ornithine decarboxylase activity in macrophages. A single injection of apoptotic cells in infected mice increases parasitaemia, whereas treatment with cyclooxygenase inhibitors almost completely ablates it *in vivo*. These results suggest that continual lymphocyte apoptosis and phagocytosis of apoptotic cells by macrophages have a role in parasite persistence in the host, and that cyclooxygenase inhibitors have potential therapeutic application in the control of parasite replication and spread in Chagas' disease.

We have already shown that the onset of activation-induced cell death in $CD4^+$ T cells exacerbates parasite replication in co-cultured macrophages infected with *T. cruzi*⁵. To investigate whether the clearance of apoptotic cells predisposes macrophages to *T. cruzi* infection, murine resident peritoneal macrophages were exposed to apoptotic, necrotic or viable splenic T cells first, and then washed and infected. Apoptotic, but not necrotic or living T cells increased *T. cruzi* growth in macrophage cultures (Fig. 1a). Similar results were obtained when apoptotic or necrotic cells were added after *T. cruzi* infection (data not shown). Nevertheless, treatment of lymphocytes with the caspase-inhibitor zVAD-fmk peptide before apoptosis induction, rescued T cells from death (data not shown) and prevented the increase in parasite replication (Fig. 1b) in a dose-dependent manner. In another model, peritoneal macrophages from mice infected with *T. cruzi* were incubated with apoptotic or necrotic cells. Apoptotic, but not necrotic cells also exacerbated endogenous *T. cruzi* growth in these *in vivo* infected macrophages (Fig. 1c). In agreement with *in vitro* results, a single *in vivo* injection of apoptotic, but not necrotic cells in *T. cruzi*-infected mice resulted in a sudden rise in parasitaemia (Fig. 1d).

Previous studies pointed to a role for an integrin in the recognition and ingestion of apoptotic cells by macrophages^{6,7}. We observed that RGDS, but not RGEs peptide blocked apoptotic cell binding and reduced *T. cruzi* growth within macrophages (data not shown).

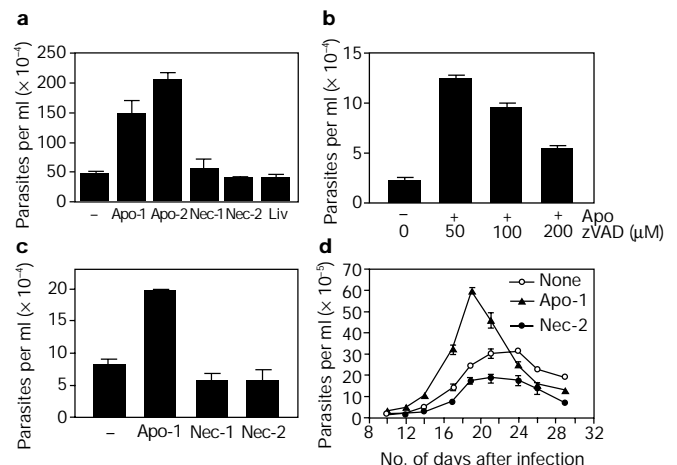


Figure 1 Apoptotic cells exacerbate parasite growth in *T. cruzi* infection. **a**, Peritoneal resident macrophages were either untreated (–) or exposed to Apo-1, Apo-2, Nec-1, Nec-2 or to living cells (Liv). After 5 days, cells were removed and macrophages were infected with *T. cruzi*; parasites were counted 10 days later. **b**, T cells (Apo) were treated with the indicated doses of zVAD-fmk (zVAD) before apoptosis induction (by heating) and added to macrophages infected *in vitro*. Parasites were counted 7 days later. Maximal cell death (100%) and increased parasite replication still occurred with zVAD-fmk at 50 μ M. **c**, Macrophages from infected mice were exposed to Apo-1, Nec-1 or Nec-2 throughout culture, and trypomastigotes counted 10 days later. **d**, Mice were injected 7 days after infection with Apo-1 or Nec-2, and parasitaemia was monitored.